

Dynamics of transparent exopolymer particles (TEP) during the VAHINE mesocosm experiment in the New Caledonia lagoon

I. Berman- Frank¹, D. Spungin¹, E. Rahav^{1,2}, F. Van Wambeke³, K. Turk-Kubo⁴, T. Moutin³

[1] {The Mina and Everard Goodman Faculty of Life Sciences, Bar-Ilan University, Ramat Gan, Israel 5290002}

[2] {National Institute of Oceanography, Israel Oceanographic and Limnological Research, Haifa, Israel 31080}

[3] {Aix Marseille Université, CNRS/INSU, Université de Toulon, IRD, Mediterranean Institute of Oceanography (MIO) UM110, 13288, Marseille, France}

[4] {Ocean Sciences Department, University of California, Santa Cruz, 1156 High Street, Santa Cruz, CA, 95064, USA}

Correspondence to: I. Berman-Frank (ilana.berman-frank@biu.ac.il)

Abstract

In the marine environment, transparent exopolymeric particles (TEP) produced from abiotic and biotic sources link the particulate and dissolved carbon pools and are essential vectors enhancing vertical carbon flux. We characterized spatial and temporal dynamics of TEP during the VAHINE experiment that investigated the fate of diazotroph-derived nitrogen and carbon in three, replicate, dissolved inorganic phosphorus (DIP)-fertilized 50 m³ enclosures in an oligotrophic New Caledonian lagoon. During the 23 days of the experiment, we did not observe any depth dependent changes in TEP concentrations in the three sampled-depths (1, 6, 12 m). TEP carbon (TEP-C) content averaged $28.9 \pm 9.3\%$ and $27.0 \pm 7.2\%$ of TOC in the mesocosms and surrounding lagoon respectively and was strongly and positively coupled with TOC during P2 (= days 15-23). TEP concentrations in the mesocosms declined for the first 9 days after DIP fertilization (P1 = days 5-14) and then gradually increased during the second phase. Temporal changes in TEP concentrations paralleled the growth and mortality rates of the diatom-diazotroph association of *Rhizosolenia* and *Richelia* that predominated the diazotroph community during P1. By P2, increasing total primary and heterotrophic bacterial production consumed the supplemented P and reduced availability of DIP. For this period, TEP concentrations were negatively correlated with DIP availability and turnover time of DIP (T_{DIP}), while positively associated with enhanced alkaline phosphatase activity (APA) that occurs when the microbial populations are P-stressed. During P2, increasing bacterial production (BP) was positively correlated with higher TEP concentrations, which were also coupled with the increased growth rates and aggregation of the unicellular UCYN-C diazotrophs that bloomed during this period. We conclude that the composite processes responsible for the formation and breakdown of TEP yielded a relatively stable TEP pool available as both a carbon source and facilitating aggregation and flux throughout the experiment. TEP was probably mostly influenced by abiotic physical processes during P1 while biological activity (BP, diazotrophic growth and aggregation, export production) mainly impacted TEP concentrations during P2 when DIP-availability was limited.

1 Introduction

The cycling of carbon (C) in the oceans is a complex interplay between physical, chemical, and biological processes that regulate the input and the fate of carbon within the ocean. An essential process driving the flux of carbon and other organic matter to depth and enabling long term sequestration and removal of carbon from the atmosphere is the biological

60 pump that drives organic C formed during photosynthesis to the deep ocean. This process,
61 termed export production (Eppley and Peterson, 1979), is facilitated via physical inputs of
62 ‘new’ nutrients (e.g. nitrogen, phosphorus, silica, trace metals, etc.) into the euphotic zone
63 from either external sources (deep mixing of upwelled water, river discharge, dust deposition,
64 and anthropogenic inputs) or via biological processes such as microbial N₂ fixation that
65 converts biologically unavailable dinitrogen (N₂) gas into bioavailable forms of nitrogen and
66 enhances the productivity of oligotrophic oceanic surface waters that are often limited by
67 nitrogen (Capone, 2001; Falkowski, 1997).

68 Marine N₂ fixation is performed by diverse prokaryotic organisms comprised
69 predominantly of autotrophic cyanobacteria and heterotrophic bacteria (Zehr and Kudela,
70 2011). To supply the energetically-expensive process of converting N₂ to ammonia
71 (Mulholland and Capone, 2000; Postgate and Eady, 1988; Stam et al., 1987), these organisms
72 must obtain energy from either photosynthesis (cyanobacteria) or from bioavailable organic
73 carbon compounds within the aquatic milieu (heterotrophic bacteria and mixotrophs). The
74 total organic carbon (TOC) in the ocean contains dynamic particulate (POC) and dissolved
75 organic carbon (DOC) pools. These are supplied by biotic sources and are broken down into
76 organic C-containing marine microgels which include transparent polymeric particles (TEP).
77 TEP are predominantly acidic polysacchridic organic particles ranging in size from ~0.45 to >
78 300 µm and are found in both marine and freshwater habitats (Passow, 2002). Both biotic and
79 abiotic processes form aquatic TEP that are routinely detected by staining with Alcian Blue
80 (Alldredge et al., 1993; Passow and Alldredge, 1995). Abiotic TEP occur by coagulation of
81 colloidal precursors in the pool of dissolved organic matter (DOM) and from planktonic
82 debris (Passow, 2002; Verdugo and Santschi, 2010) that may be stimulated by turbulence or
83 by bubble adsorption (Logan et al., 1995; Passow, 2002; Zhou et al., 1998). Biotically TEP
84 form from extracellular excretion or mucilage in algae and bacteria and from grazing and
85 microbial breakdown of larger marine snow particles [reviewd in (Bar-Zeev et al., 2015;
86 Passow, 2002)].

87 TEPs are light and bouyant (Azetsu-Scott and Passow, 2004). Yet, once formed, TEPs
88 sticky nature enhances and consolidates the formation of larger aggregates such as
89 marine/lake snow providing favorable environments for diverse microorganisms (Engel,
90 2004; Passow, 2002). Sedimentation of TEP associated “hot spots” from the surface are
91 important for transporting particulate organic material and microorganisms to deeper waters
92 (Azam and Malfatti, 2007; Bar-Zeev et al., 2009; Smith and Azam, 1992). During

sedimentation, TEP can also function as a direct source of carbon and other nutrients for higher trophic level organisms such as protists, micro-zooplankton, and nekton (Engel, 2004; Passow, 2002).

TEP production can be enhanced in late phases of algal blooms and in senescent or nutrient-stressed phytoplankton (Berman-Frank et al., 2007; Engel, 2004; Grossart et al., 1997; Passow, 2002). Thus, TEP in oligotrophic waters provide a source of available carbon to fuel microbial food webs (Azam and Malfatti, 2007) that typically succeed autotrophic blooms. TEP based aggregates or marine snow containing TEP typically with high carbon (C): nitrogen (N) ratios (Berman-Frank and Dubinsky, 1999; Wood and Van Valen, 1990), which can also fuel N₂ fixation by heterotrophic diazotrophs both in oxygenated surface waters and in the aphotic zones (Benavides et al., 2015; Rahav et al., 2013).

The VAHINE project was designed to examine the fate/s of ‘newly’-fixed N by diazotrophs or diazotroph-derived N (hereafter called DDN) in the pelagic food web using large mesocosms in the oligotrophic tropical lagoon of New Caledonia where diverse diazotrophic populations have been observed (Biegala and Raimbault, 2008; Bonnet et al., 2016; Dupouy et al., 2000; Garcia et al., 2007; Rodier and Le Borgne, 2008; Rodier and Le Borgne, 2010). One of the major questions addressed during VAHINE was whether diazotroph blooms significantly modify the stocks, fluxes, and ratios of biogenic elements (C, N, P, Si) and the efficiency of carbon export. To this end, the 3 large-volume (~50 m³) mesocosms containing ambient lagoon waters were fertilized with 0.8 μmol L⁻¹ DIP, and multiple parameters were measured inside and outside of the mesocosms for 23 days [details of parameters and experimental setup in Bonnet et al. (2016)]. Within the VAHINE framework, our specific objectives were: 1) to examine the spatial and temporal dynamics of TEP; 2) to determine whether TEP content was regulated by nutrient status in the mesocosms - specifically DIP availability; 3) to examine the relationship between TEP content, particulate and dissolved carbon, and primary or heterotrophic bacterial production; and 4) to elucidate whether TEP provided a source of energy for diazotrophs/bacteria/mixotrophs in mesocosms.

2 Methods

2.1 Study site, mesocosm description, and sampling strategy

Three large-volume (~50 m³) mesocosms were deployed at the exit of the oligotrophic New Caledonian lagoon (22°29.10 S–166°26.90 E), from 13 January 2013 (day 1) to 4 February

2013 (day 23). The complete description of the mesocosm design and deployment, as well as the sampling strategy, is detailed in Bonnet et al. (2016). The mesocosms were supplemented with $0.8 \mu\text{mol L}^{-1} \text{KH}_2\text{PO}_4$ (hereafter referred to as DIP fertilization) between day 4 and 5 day of the experiment to promote N_2 fixation. Samples were collected during the early morning of each day for 23 days with a clean Teflon pumping system from 3 selected depths (1 m, 6 m, 12 m) in each mesocosm (M1, M2 and M3) and outside (hereafter called 'lagoon waters'-O). Based on the results of different biogeochemical and biological parameters during VAHINE (Berthelot et al., 2015; Bonnet et al., 2015; Turk-Kubo et al., 2015), three specific periods were discerned (see detailed description in section 3.1) within which we have also investigated TEP dynamics: Days 2-4 (P0) are the pre-fertilization days when the DIP concentrations were $0.02\text{-}0.05 \mu\text{mol L}^{-1} \text{PO}_4^{3-}$ and combined DIN were extremely low; days 5-14 (P1) –After fertilization on day 5 the PO_4^{3-} concentrations were $\sim 0.8 \mu\text{mol L}^{-1}$ and diazotrophic populations were dominated by diatom-diazotroph associations. The second stage of the experiment (P2) from days 15 to 23 was characterized by simultaneous increase in primary and bacterial production as well as in N_2 fixation rates which averaged $27.7 \text{ nmol N L}^{-1} \text{d}^{-1}$ (Berthelot et al., 2015) and diazotrophic populations comprised primarily by the unicellular UCYN-C (Turk-Kubo et al., 2015).

2.2 TEP quantification

Water samples (100 mL) were gently ($< 150 \text{ mbar}$) filtered through a $0.45 \mu\text{m}$ polycarbonate filters (GE Water & Process Technologies). Filters were then stained with a solution of 0.02% Alcian Blue (AB) and 0.06% acetic acid (pH of 2.5). The excess dye was removed by a quick deionized water rinse. Filters were then immersed in sulfuric acid (80%) for 2 h, and the absorbance at 787 nm was measured spectrophotometrically (CARY 100, equipped with an integrated sphere, Varian). AB was calibrated using different volumes of purified polysaccharide GX (Passow and Alldredge, 1995). TEP concentrations ($\mu\text{g gum xanthan [GX] equivalents L}^{-1}$) were measured according to Passow and Alldredge, (1995). Total TEP content in the mesocosms was calculated by integrating the weighted average of the TEP concentrations per depth and multiplying by the specific volume of each mesocosm. To estimate the role of TEP in C cycling, total amount of TEP-C was calculated for each mesocosm, using the volumetric TEP concentrations at each depth, the specific volume per mesocosm, and the conversion of GX equivalents to carbon applying the revised factor of 0.63 based on empirical experiments from both natural samples from different oceanic areas and phytoplankton cultures (Engel, 2004).

2.3 Total Organic Carbon (TOC), Particulate Organic Carbon (POC), Dissolved Organic Carbon (DOC)

Samples for TOC concentrations were collected in duplicate from 6 m in each mesocosm and in lagoon waters in precombusted sealed glassware flasks, acidified with H_2PO_4 and stored in the dark at 4 °C until analysis. Samples were analyzed on a Shimadzu TOCV analyzer with a typical precision of $2 \mu\text{mol L}^{-1}$. Samples for POC concentrations were collected by filtering 2.3 L of seawater through a precombusted GF/F filter (450 °C for 4 h), combusted and analyzed on an EA 2400 CHN analyzer. DOC concentrations were calculated as the difference between TOC and POC concentrations. Fully detailed methodologies and data are available in Berthelot et al. (2015).

2.4 Dissolved inorganic phosphorus (DIP) and alkaline phosphatase activity (APA)

The determination of DIP concentrations are detailed in Berthelot et al. (2015). Samples for DIP were collected from each of the three depths in M1, M2 and M3 and lagoon waters (O) in 40 mL glass bottles, and stored in -20 °C until analysis. DIP concentration was determined using a segmented flow analyzer according to Aminot and K  rouel (2007). The alkaline phosphatase activity (APA) was measured from the same depths and sites using the analog substrate methylumbelliferone phosphate (MUF-P, 1 μM final concentration; SIGMA), (Hoppe, 1983). Full details of the measurements and analyses are described in Van Wambeke et al. (2015).

2.5 Chlorophyll a (Chl a), Primary production (PP) and DIP turnover time

Chlorophyll a (Chl a) concentrations were determined by the non-acidification method as described in Berthelot et al. (2015). Primary production (PP) rates and DIP turnover time (T_{DIP} , i.e., the ratio of PO_4^{3-} concentration and uptake) were measured using the $^{14}\text{C}/^{33}\text{P}$ dual labeling method (Duhamel et al., 2006). 60 mL bottles were amended with ^{14}C and ^{33}P and incubated for 3 to 4 h under ambient light and temperature. This was followed by the addition of 50 μL of KH_2PO_4 solution (10 mmol L^{-1}) to stop ^{33}P assimilation. Samples were then kept in the dark to stop ^{14}C uptake. Samples were filtered on 0.2 μm polycarbonate membrane filters, and counts were done using a Packard Tri-Carb   2100TR scintillation counter. PP and T_{DIP} were calculated according to Moutin et al. (2002).

2.6 Bacterial production (BP)

Heterotrophic bacterial production (BP) was estimated using the ^3H -leucine incorporation technique (Kirchman, 1993), adapted to the centrifuge method (Smith and Azam, 1992). The complete methodology including enumeration of heterotrophic bacterial abundances (BA) by flow cytometry is detailed in Van Wambeke et al. (2015).

2.7 N_2 fixation, diazotrophic abundance and growth rates

N_2 fixation rates were determined daily on ambient waters from mesocosms and the lagoon. Samples were spiked with 99% $^{15}\text{N}_2$ -enriched seawater (Mohr et al., 2010), incubated *in situ* under ambient light and seawater temperatures as detailed in Berthelot et al. (2015) and Bonnet et al. (2015).

Data and protocols of sampling for diazotrophic abundance and calculation of their respective growth rates are detailed fully in Turk-Kubo et al. (2015). Briefly, samples (from 6 m only) were collected every other day from the mesocosms, and from the lagoon waters. DNA was extracted and nine diazotrophic phylotypes were identified using quantitative PCR (qPCR). The targeted diazotrophs were two unicellular diazotrophic symbionts of different *Braarudosphaera bigelowii* strains, UCYN-A1, UCYN-A2; free-living unicellular diazotroph cyanobacterial phylotypes UCYN-B (*Crocospaera* sp.), and UCYN-C (*Cyanothece* sp. and relatives); *Trichodesmium* spp.; and three diatom-diazotroph associations (DDAs), *Richelia* associated with *Rhizosolenia* (Het-1), *Richelia* associated with *Hemiaulus* (Het-2), *Calothrix* associated with *Chaetoceros* (Het-3), and a widespread gamma-proteobacterial phylotype γ -24774A11. Abundances are reported as *nifH* copies L^{-1} as the number of *nifH* copies per genome in these diazotrophs are uncertain. Growth and mortality rates were calculated for individual diazotrophs inside the mesocosms when abundances were higher than the limit of quantification (LOQ) for two consecutive sampling days as detailed in Turk-Kubo et al. (2015).

2.8 Microscopic Analyses

Detailed method for sampling for microscopic analyses is described in Bonnet et al., (2015). Phytoplankton were visualized using a Zeiss Axioplan (Zeiss, Jena, Germany) epifluorescence microscope fitted with a green (510-560 nm) excitation filter, which targeted the *Richelia* and the UCYN phycoerythrin-rich cells. The diatom-diazotroph association *Rhizosolenia*-*Richelia* were imaged in bright-field.

2.9 Statistical analyses

Statistical analyses were carried out with XLSTAT, a Microsoft Office Excel based software. A Pearson correlation coefficient test was applied to examine the association between two variables (TEP versus physical, chemical, or physiological variable) after linear regressions or log-transformation of the data. The non-parametric Kruskal–Wallis one-way analysis of variance was applied to compare between TEP dynamics from each of the different phases. A confidence level of 95% (α - 0.05) was used. More details can be found in the supporting information.

3 Results and Discussion

3.1 General context and spatial and temporal dynamics of TEP

The VAHINE experiment was designed to induce and follow diazotrophic blooms and their fate within an oligotrophic environment (Bonnet et al., 2016). Our specific objectives of investigating TEP dynamics were thus examined within the general context and aims of the large experiment. The first stage of the experiment involved the enclosure of the lagoon waters and 3 days of equilibration of the system (P0 – pre-fertilization days 2-4). At this initial stage the total Chl *a* concentrations averaged around 0.2 $\mu\text{g L}^{-1}$ in the lagoon water and in the mesocosms and the phytoplankton consisted of diverse representatives from the cyanobacteria (*Prochlorococcus*, *Synechococcus*, and diatoms such as *Pseudosolenia calcar-avis* (Leblanc et al., 2016). During P0, the most abundant members of the diazotrophic community in the lagoon waters were *Richelia-Rhizosolenia* (Het-1), the unicellular UCYN-A1, UCYN-A2, UCYN-C, and the filamentous *Trichodesmium* (Turk-Kubo et al., 2015).

Fertilization of the mesocosms with DIP on day 4 stimulated a two-stage response by the diazotrophic community that was further reflected by many of the measured chemical and biological parameters (Berthelot et al., 2015; Bonnet et al., 2015; Bonnet et al., 2016; Turk-Kubo et al., 2015). After fertilization, from day 5 through day 14 (P1), excluding a significant increase in N_2 fixation rates, the functional community-wide biological responses (Chl *a*, PP, BP, BA) remained relatively low and similar to the values for P0 and for P1 in the outside lagoon waters (Berthelot et al., 2015; Leblanc et al., 2016; Van Wambeke et al., 2015). The autotrophic community during P1 was comprised of picophytoplankton such as *Prochlorococcus* *Synechococcus*, micro and nanophytoplankton including dinoflagellates, and a diverse diatom community (*Chaetoceros*, *Leptocylindrus*, *Cerataulina*, *Guinardia*, and

Hemiaulus), (Leblanc et al., 2016). Diatom-diazotroph associations (DDAs), predominantly *Richelia-Rhizosolenia* (Het-1) dominated the diazotroph community in the mesocosms (Turk-Kubo et al., 2015) although it still only contributed from 2% to ~8% of the total diatom biomass in P0 and P1 respectively (Leblanc et al., 2016). These DDAs were succeeded during the last 9 days (day 15 to 23 termed P2) by a large bloom of unicellular diazotrophs characterized predominantly as UCYN-C (Turk-Kubo et al., 2015).

The final stage of the experiment (P2, days 15-23) was characterized by significantly enhanced values for many biological parameters including N₂ fixation rates, Chl *a*, PP, BA, BP, and particulate organic carbon and nitrogen compared to their respective average values in P1 (Bonnet et al., 2015; Leblanc et al., 2016; Van Wambeke et al., 2015). In all three mesocosms, a significant bloom of UCYN-C developed (day 11 – M1, day 13-M2, day 15-M3) and remained dominant representatives of the diazotroph community until day 23 (Turk-Kubo et al., 2015). The ambient autotrophic community responded to the input of new N, and the transfer of diazotroph derived N was demonstrated and seen in increasing abundance of *Synechococcus*, pico-eukaryotes, and the non-diazotrophic diatoms *Navicula* and *Chaetoceros* spp. (Bonnet et al., 2015; Leblanc et al., 2016; Van Wambeke et al., 2015). Thus the extremely high N₂ fixation rates during this experiment provided sufficient new N to yield high Chl *a* concentrations (> 1.4 µg L⁻¹) and rates of PP (> 2 µmol C L⁻¹ d⁻¹) (Berthelot et al., 2015).

3.1.1 Dynamics of TEP

TEP concentrations for the entire experimental period ranged from ~22 to 1200 µg GX L⁻¹. In each mesocosm and in the lagoon waters (O), the TEP concentrations were similar for the three sampled depths within the 15 m water-column with an overall average of 350 ± 180 µg GX L⁻¹ (Fig. S1). Temporally, TEP concentrations generally followed the three distinct periods (P0, P1, P2) that coincided with the described experimental phases characterized from the diazotrophic populations and the biogeochemical and biological (production) parameters (Berthelot et al., 2015; Bonnet et al., 2015; Leblanc et al., 2016; Turk-Kubo et al., 2015; Van Wambeke et al., 2015) (Fig. 1, Fig. S1). Following the enclosure of the lagoon water in the mesocosms (day 2), TEP concentrations increased from the lowest volumetric concentrations (averaging ~ 50 µg GX L⁻¹) measured on day 2 to reach maximum concentrations in each of the mesocosms (average of ~ 800 µg GX L⁻¹) on day 5, ~ 15 h after the mesocosms were fertilized with DIP (Fig. S1, Fig. 1a). From day 5 to day 14 (P1) average TEP content in M2

and M3 decreased slightly yet significantly ($p < 0.05$) with the major decline in all mesocosms measured from day 5 to 6 (Fig. 1, Fig. S1, Table S1). From day 15 to 23 (P2) TEP concentrations in all mesocosms increased gradually ($p < 0.05$) over the subsequent 9 days to reach $381 \pm 39 \mu\text{g GX L}^{-1}$ on day 23 (Fig. 1, Table S1).

TEP concentrations in the lagoon waters were compared with those in the mesocosms. These showed a similar pattern of increase in TEP during P0 and P2 while the gradual decline in TEP concentrations during P1 was not statistically significant as observed in the mesocosms (Fig. 1, Fig. S1). In the lagoon waters, average TEP concentrations over the whole experimental period day 2 to day 23 were $335 \pm 56 \mu\text{g GX L}^{-1}$. While temporal variations in the three mesocosms were generally statistically significant (Fig. 1, Table S1), the total TEP content calculated for each mesocosm and for an equivalent volume of lagoon water based on average mesocosm volume did not differ significantly when we assessed all data obtained during P1 and P2 (Fig. 2, $p > 0.05$, Kruskal –Wallis analyses of variance). The lack of significant differences in total TEP content in the mesocosms throughout the experiment could reflect the contrasting processes of formation and breakdown that together maintain a relatively stable pool of available TEP.

Mechanical processes such as wave turbulence and tidal effects can influence TEP formation and breakdown (and resulting content), (Passow, 2002; Stoderegger and Herndl, 1999). Our results indicate no obvious effects of these parameters on TEP content as these were similar in the enclosed mesocosms and the outside lagoon (Fig. 1, Fig. 2). The difference between the TEP in the mesocosms and the lagoon water is significantly different immediately after P addition and only during P1 after P addition and subsequent utilization when declining P availability was correlated with increased TEP concentrations in the mesocosms. TEP concentrations from the lagoon water during P1 did not show any significant trend (Fig. 1, Fig. S1). In the mesocosms, the significant decline in TEP in the first days after P addition is probably due to two factors: a) phytoplankton relieved of P stress will produce less TEP and increase growth rates, b) bacteria will utilize the added P as well as TEP and other organic C sources to grow – so higher TEP consumption and therefore a more significant decline in the mesocosms compared to the outside lagoon, (see below section 3.2).

The relative uniformity and stability of TEP within the 15 m water column of both the mesocosms and the lagoon waters reflects the homogeneity of the shallow lagoon system. The variability between the three depths was statistically insignificant in many of the other physical, chemical, and biological features of the mesocosms and the lagoon waters for

temperature, salinity, inorganic nutrients (N, P, Si), POC, PON, POP, DOC, Chl *a*, and primary production and heterotrophic bacterial production (Berthelot et al., 2015; Bonnet et al., 2015; Bonnet et al., 2016; Van Wambeke et al., 2015). In contrast to some marine systems where TEP concentrations were correlated with the vertical distribution of Chl *a* or POC (Bar-Zeev et al., 2009; Bar-Zeev et al., 2011; Engel, 2004; Ortega-Retuerta et al., 2009; Passow, 2002), the results we obtained here showed no correlation to the vertical (i.e. depth related) autotrophic signatures. Moreover, the similar TEP concentrations at 1, 6, and 15 m do not support a sub-surface maxima in TEP concentrations, stimulated by abiotic aggregation, at the sea-surface top layer as has been reported at 1 m depth in different oceanic areas (Wurl et al., 2011). Abiotic processes of formation and breakdown can be influential yet here we do not see a depth-correlated specific abiotic driver and TEP were evenly distributed within the 15 m water column for all mesocosms (Fig. S1).

3.2 DIP availability, APA, and TEP content.

The average TEP concentrations we measured in the New Caledonian waters are comparable to TEP concentrations reported from other marine environments such as the eastern temperate-subarctic North Atlantic (Engel, 2004), the Ross Sea (Hong et al., 1997), western Mediterranean – Gulf of Cadiz and the Straits of Gibraltar (García et al., 2002; Prieto et al., 2006), the Gulf of Aqaba (northern Red Sea), (Bar-Zeev et al., 2009), in the northern Adriatic Sea (Radić et al., 2005), and in the New Caledonia lagoon (Mari et al., 2007; Rochelle-Newall et al., 2008).

While prediction as to the expected TEP concentrations with trophic or productive status is difficult (Beauvais et al., 2003), decreasing availability of dissolved nutrients such as nitrate and phosphate have been correlated with enriched TEP concentrations in both cultured phytoplankton and natural marine systems (Bar-Zeev et al., 2011; Brussaard et al., 2005; Engel et al., 2002; Urbani et al., 2005). In P-limited systems, low Chl *a* concentrations often reflect the nutrient-stressed phytoplankton. As long as light and CO₂ are available, limitation of essential nutrients results in an uncoupling between carbon fixation and growth during which the excess photosynthate can be used to produce carbon-rich compounds including TEP (Berman-Frank and Dubinsky, 1999; Mari et al., 2001; Rochelle-Newall et al., 2008). Moreover, as DIP-availability declines, cells activate P-acquisition pathways and enzymes such as APA to access P from other sources. Thus, and based on previous data (Bar-Zeev et

al., 2011), we hypothesized that TEP content would be negatively correlated with autotrophic biomass (Chl *a*) and PP and positively correlated with APA.

Mesocosm fertilization on the evening of day 4 enriched the system with ten-fold higher DIP concentrations that were available for microbial utilization throughout the following 8 – 10 days (Berthelot et al., 2015; Bonnet et al., 2016; Leblanc et al., 2016; Van Wambeke et al., 2015). Thus, when DIP concentrations were relatively sufficient during P1, no statistically significant relationship was observed between TEP and POP, DIP, T_{DIP} , Chl *a*, or PP (Table S2). This situation changed with the declining availability of DIP and the shift in the response of the system during P2 from day 15 to 23. During P2 high TEP concentrations were associated with decreasing DIP for each of the mesocosms with an overall negative correlation ($R^2 = 0.23$, $n = 23$, $p = 0.02$), (Fig. 3a). A similar negative trend was obtained between TEP and the turnover time of DIP (T_{DIP}) ($R^2 = 0.28$ $n = 26$, $p = 0.006$), (Fig. 3b).

In the South West Pacific, the critical DIP turnover time (T_{DIP}) required for single filaments of *Trichodesmium* to grow is 2 d (Moutin et al., 2005). Here T_{DIP} values lower than 1 d, indicative of a strong DIP deficiency, were reached on day 14 in M1, day 19 for M2, and on day 21 for M3. The average T_{DIP} values during P2 were significantly different in each mesocosm, T_{DIP} of 0.5, 1.8, 3.9 d for M1, M2, M3, respectively (Berthelot et al., 2015). Although turnover rates alone do not indicate P deficiency, increasing alkaline phosphatase activity (APA) suggests that the cells were responding to P stress. APA increased rapidly in both M1 and M2 from day 18 (average for M1 and M2 during P2 $\sim 8 \pm 6$ nmol MUF L⁻¹ h⁻¹) and after day 21 in M3 illustrating a biological response of the microbial community to P stress (Van Wambeke et al., 2015). We did not specifically measure TEP production by autotrophic or heterotrophic plankton. Yet, the significant (although indirect relationship) negative correlation of TEP with DIP concentrations and T_{DIP} (Fig. 3a-b) suggests that microbial responses to decreased DIP availability resulted from either 1) an increase in TEP synthesis through higher polysaccharide production rather than biomass which requires higher nutrients (Berman-Frank and Dubinsky, 1999; Wood and Van Valen, 1990) or 2) nutrient limitation inducing greater breakdown of biomass and POM (maybe via programmed cell death) and subsequent abiotic formation of TEP. We obtained a significant semi-logarithmic relationship between TEP and APA ($R^2 = 0.33$ $n = 25$, $p = 0.002$), (Fig. 3c) which implies active TEP formation when DIP concentrations are reduced and APA increases until a saturating point whereby any further increases in APA do not appear to impact TEP concentrations (Fig. 3c). This relationship may not always be valid as APA in the lagoon

waters was consistently higher at 1 m than APA measured at 6 and 12 m depths (Van Wambeke et al., 2015), yet TEP concentrations were uniform at all depths (Fig. S1).

3.3 TEP and carbon pools

The size range of TEP spans a range of particles from 0.45 to 300 μm (Alldredge et al., 1993; Bar-Zeev et al., 2015). TEP precursors (0.05 to 0.45 μm size) are formed and broken down in the DOC pool and thus essentially “TEP establish a bridge between DOM (including DOC) and the POM pool” (Engel, 2004). Our data shows a generally stable contribution of TEP to the TOC pool. Excluding day 5, where TEP-C comprised $56.5 \pm 8\%$ of TOC, the % TEP-C was $28.9 \pm 9.3\%$ and $27.0 \pm 7.2\%$ of the TOC in all mesocosms and in the lagoon waters, respectively (Fig. 4a-b).

TEP concentrations can be directly and positively correlated with POC (Engel, 2004) and with DOC (Ortega-Retuerta et al., 2009). Yet, TEP concentrations can also be negatively related to POC indicative of low TEP production when POC concentrations are high (Bar-Zeev et al., 2011). In the mesocosms, a significant positive correlation between TEP concentrations and TOC was obtained for all three mesocosms only during P2 ($R^2 = 0.75$, 0.73, 0.58 and $p < 0.05$ for M1, M2, M3 respectively), (Fig. 4c, Table S2). This period coincided with the largest gain in total autotrophic and heterotrophic biomass and elevated N_2 fixation, PP, and BP rates (Berthelot et al., 2015; Bonnet et al., 2015; Van Wambeke et al., 2015).

Although TEP was significantly and positively correlated with TOC in the mesocosms during P2, this was not the case in the Lagoon water (outside the mesocosms) (Table S2) or with either POC or DOC in any mesocosm for either P1 or P2 (Table S2). The absence of any significant correlation between TEP and POC was surprising as TEP are part of the POC pool comprising 40 – 60% of the particulate combined carbohydrates in POC (Engel, 2004; Engel et al., 2012). Furthermore, we did not obtain any significant correlations of TEP and specific components of the dissolved organic matter such as fluorescent dissolved organic matter (FDOM) or chromophoric dissolved organic matter (CDOM) that was coupled to the dynamics of N_2 fixation in the mesocosms (Tedetti et al., 2015). The lack of significant correlation could partially reflect methodological issues. In this experiment [and operationally according to published protocol (Passow and Alldredge (1995))] TEP was measured on 0.45 μm filters – so that Alcian Blue stained particles included particles $> 0.45 \mu\text{m}$ while POC was measured on GF/F (nominal pore size 0.7 μm). DOC is typically considered for the $< 0.45 \mu\text{m}$

fraction (Thurman, 1985), although here no direct measurements of DOC were made and DOC was obtained by subtracting POC from TOC. Thus, DOC actually covered the $< 0.7 \mu\text{m}$ fraction. Our methodology therefore precluded determination of the smaller TEP precursors that would contribute to the DOC and colloidal pools (Villacorte et al., 2015). As such we probably overestimated TEP relative to POC and at the same time underestimated TEP's contribution to the DOC pool (Bar-Zeev et al., 2009). The lacking correspondence between TEP concentrations and the pools of POC and DOC may also result from the uncoupling between formation and breakdown processes. Abiotic processes, will modify relationships obtained between biotic TEP production and recycling (Wurl et al., 2011). Thus, it is feasible that especially during P1 abiotic factors predominated breaking down larger TEP particles into smaller TEP precursors that would be mobilized to the DOC pool and would thus maintain a relatively stable TEP pool although we observed a positive increase in TEP with increased blooms of DDAs (see below section 3.4.1).

3.4 Production and utilization of TEP by primary and bacterial populations

Typically TEP are formed by diverse algal and bacterial species (Mari and Burd, 1998) yet are utilized mostly by bacteria and grazers as a rich C source (Azam and Malfatti, 2007; Bar-Zeev et al., 2015; Engel and Passow, 2001). Throughout this experiment (P1 and P2 stages) TEP was not significantly correlated to parameters related to autotrophic production such as total Chl *a*, PP, non-diazotrophic diatom or cyanobacterial abundance, or the growth and mortality rates of these populations (Table S2). Furthermore, during P1, no significant relationship between TEP and BA (total or specific for high and low nucleic acid bacteria-HNA or LNA respectively), BP, or division rates was noted in any of the mesocosms (Table S2).

This changed during P2 when TEP was positively correlated to the increasing BP for all three mesocosms (Pearson's correlation coefficient $R^2 = 0.63, 0.66, 0.69$ for M1, M2, and M3 respectively, $p < 0.05$), (Fig. 5). This contrasted with the relationship in the lagoon water outside the mesocosms where no significant correlation between TEP and BP was noted (Table S2) During P2, TEP was also strongly and positively correlated to TOC, which significantly increased over this time period (Fig. 4c) due to the high production rates of both photosynthetic and heterotrophic bacterial populations. However, although BP and PP were positively associated during P2 [log-log transformation, Fig. 5 and in Van Wambeke et al. (2015)], we found no direct correlation between TEP and PP for either linear (Table S2) or

log-transformed regression (not shown). This coupling between PP and BP, while a concurrent association between TEP and BP occurred during P2, indicates TEP may have been utilized by bacteria as a carbon source (Azam, 1998; Ziervogel et al., 2014) or provided a suitable niche for aggregation and proliferation of heterotrophic bacteria.

3.4.1 TEP and diazotrophic populations

Overall N₂ fixation rates were not significantly correlated with TEP concentrations at any time in the experiment (Table S2). Neither could we discern any direct evidence of TEP providing a carbon source for heterotrophic diazotrophs as was found previously in the Gulf of Aqaba where these organisms contributed greatly to the N₂ fixation rates (Rahav et al., 2015). Indeed, no relationship was found between TEP concentrations and the abundance or growth rates of the heterotrophic diazotrophs γ -24774A11 (Moisander et al., 2014). Although these organisms were present throughout the experiment, and increased ~ 4 fold from day 9 to 15 especially in M3, they contributed only a small fraction to the total diazotrophic biomass and N₂ fixation rates (Turk-Kubo et al., 2015).

Yet, discerning individual diazotroph populations revealed some species-specific correspondence to TEP at certain periods during the experiment. For example, throughout the experiment, net growth rates (i.e., based on differences of *nifH* copies L⁻¹ from day to day) of the DDA *Richelia* (Het-1) associated with *Rhizosolenia* (Turk-Kubo et al., 2015) temporally paralleled TEP concentrations in all mesocosms (Fig. 6a-c, Fig. 6e-f). During both P1 and P2 TEP concentrations were positively correlated with the net growth rates of Het-1 ($R^2=0.6$ $P = 0.0001$, $n = 19$ for all mesocosms (Fig. 6d). Although the DDAs dominated the diazotroph community during P1 (primarily Het-1), their overall contribution to diatom biomass in the mesocosm was low with only 2-8% of all diatom biomass (Leblanc et al., 2016). We did not observe an overall relationship between TEP and total diatom biomass throughout VAHINE although diatoms are well known for their TEP production especially when nutrients are limiting and growth rates decline (Fukao et al., 2010; Urbani et al., 2005). Thus, the positive association between TEP and the growth rates of Het-1 and not of the other DDAs Het-2 and Het-3 is intriguing.

TEP was also associated with the growth rates of the unicellular UCYN-C diazotrophs that bloomed during P2 and dominated the N₂ fixation rates of this period (Berthelot et al., 2015; Turk-Kubo et al., 2015). During P2, UCYN-C net growth rates were positively correlated with increasing TEP concentrations ($R^2 = 0.65, 0.83, 0.88$ for M1, M2, M3

respectively, $p < 0.05$). Furthermore, UCYN-C probably produced an organic matrix possibly also comprised of TEP that aided the formation of large aggregates (100-500 μm) (Fig. 6g-h). These aggregates were predominantly responsible for the enhanced export production ($22.4 \pm 5\%$ of exported POC), (Bonnet et al., 2015; Knapp et al., 2015). High TEP content was obtained from sediment traps on days 15 and 16 (Fig. S1), corresponding to the height of the UCYN-C bloom in the mesocosms (Turk-Kubo et al., 2015) and substantiating the role of TEP in facilitating export flux in the New Caledonia lagoon (Mari et al., 2007).

4 Conclusions

Although physically separated from the surrounding lagoon, TEP formation and breakdown was difficult to tease out in the VAHINE mesocosms where abiotic drivers (turbulence, shear forces, chemical coagulation) and biotic processes (algal and bacterial production and utilization) maintained an apparently constant pool of TEP within the TOC. Total TEP content was generally stable throughout the experimental period of 23 days and comprised $\sim 28\%$ of the TOC in the mesocosms and lagoon with uniform distribution in the three sampled depths of the 15 m deep-water column.

TEP concentrations appeared to be impacted indirectly via changes in DIP availability as it was biologically consumed in the mesocosms after fertilization. Thus, declining P availability (low DIP, rapid T_{DIP} , and increased APA) was associated with higher TEP content in all mesocosms. TEP concentrations were also positively associated with net growth rates of two important diazotrophic groups: the DDA *Richelia-Rhizosolenia* (Fig. 6e-f), during P1 and P2 (excluding days 21-23); and UCYN-C diazotrophs which bloomed during P2. High TEP content in the sediment traps during the UCYN-C bloom indicates that TEP may have been part of the organic matrix associated with the large aggregates of UCYN-C that were exported to the sediment traps (Fig. 6g-h).

TEP may have also provided bacteria with a rich organic carbon source especially during P2 when higher BP (stimulated by the higher PP) was positively correlated higher TEP concentrations. High production of TEP also occurred in the lagoon water outside the mesocosms on day 23 during the decline of a short-lived dense surface bloom of the diazotrophic *Trichodesmium* (Spungin et al., 2016). Our results emphasize the complexities of the natural system and suggest that to understand the role of compounds such as TEP, and their contribution to the DOC and POC pools, a wider perspective and methodologies should

be undertaken to examine and characterize the different components of marine gels (not only carbohydrate-based) (Bar-Zeev et al., 2015; Verdugo, 2012)

Author contributions

IBF conceived and designed the investigation of TEP dynamics within the VAHINE project. TM, FVW, IBF, DS, and ER participated in the experiment and performed analyses of samples and data, KTK analysed diazotrophic populations. IBF and DS wrote the manuscript with contributions from all co-authors.

Acknowledgements

Many thanks to Sophie Bonnet who created, designed, and successfully executed the VAHINE project. The participation of IBF, DS, and ER in the VAHINE experiment was supported by the German-Israeli Research Foundation (GIF), project number 1133-13.8/2011 to IBF, through a collaborative grant to IBF and SB from MOST Israel and the High Council for Science and Technology (HCST)-France, and United States-Israel Binational Science Foundation (BSF) grant No. 2008048 to IBF. Funding for this research was provided by the Agence Nationale de la Recherche (ANR starting grant VAHINE ANR-13-JS06-0002), INSU-LEFE-CYBER program, GOPS, IRD and M.I.O. The authors thank the captain and crew of the R/V Alis; the SEOH divers service from the IRD research center of Noumea (E. Folcher, B. Bourgeois and A. Renaud) and from the Observatoire Océanologique de Villefranche-sur-mer (OOV, J.M. Grisoni), the technical service and support of the IRD research center of Noumea. Thanks also to C. Guieu, F. Louis and J.M. Grisoni from OOV for mesocosm design and deployment advice. Special thanks to H. Berthelot and all other participants and PIs of the project for the joint efforts and for making their data available for further analyses and to the reviewers who helped improve the manuscript. This work is in partial fulfillment of the requirements for a PhD thesis for D. Spungin at Bar Ilan University.

539 **References**

- 540 Alldredge, A. L., Passow, U., and Logan, B. E.: The abundance and significance of a class of
541 large, transparent organic particles in the ocean., *Deep Sea Research*, 40, 1131-1140, 1993.
- 542 Aminot, A., and K  rouel, R.: Dosage automatique des nutriments dans les eaux marines:
543 m  thodes en flux continu, Editions Quae, 2007.
- 544 Azam, F.: Microbial control of oceanic carbon flux: The plot thickens., *Science*, 280, 694-
545 696, 1998.
- 546 Azam, F., and Malfatti, F.: Microbial structuring of marine ecosystems, *Nature Reviews*
547 *Microbiology*, 5, 782-791, 2007.
- 548 Azetsu-Scott, K., and Passow, U.: Ascending marine particles: significance of transparent
549 exopolymer particles (TEP) in the upper ocean., *Limnol. & Oceanogr*, 49, 741-748, 2004.
- 550 Bar-Zeev, E., Berman-Frank, I., Liberman, B., Rahav, E., Passow, U., and Berman, T.:
551 Transparent exopolymer particles: Potential agents for organic fouling and biofilm formation
552 in desalination and water treatment plants, *Desalination and Water Treatment*, 3, 136-142,
553 2009.
- 554 Bar-Zeev, E., Berman, T., Rahav, E., Dishon, G., Herut, B., Kress, N., and Berman-Frank, I.:
555 Transparent exopolymer particle (TEP) dynamics in the eastern Mediterranean Sea, *Marine*
556 *Ecology-Progress Series*, 431, 107-118, 10.3354/meps09110, 2011.
- 557 Bar-Zeev, E., Passow, U., Romero-Vargas Castrill  n, S., and Elimelech, M.: Transparent
558 exopolymer particles: from aquatic environments and engineered systems to membrane
559 biofouling, *Environmental science & technology*, 49, 691-707, 2015.
- 560 Beauvais, S., Pedrotti, M. L., Villa, E., and Lemee, R.: Transparent exopolymer particle
561 (TEP) dynamics in relation to trophic and hydrological conditions in the NW Mediterranean
562 Sea, *Marine Ecology-Progress Series*, 262, 97-109, 2003.
- 563 Benavides, M., Moisander, P. H., Berthelot, H., Dittmar, T., Grosso, O., and Bonnet, S.:
564 Mesopelagic N₂ Fixation Related to Organic Matter Composition in the Solomon and
565 Bismarck Seas (Southwest Pacific), *PLoS ONE*, 10, e0143775,
566 10.1371/journal.pone.0143775, 2015.
- 567 Berman-Frank, I., and Dubinsky, Z.: Balanced growth in aquatic plants: Myth or reality?
568 Phytoplankton use the imbalance between carbon assimilation and biomass production to their
569 strategic advantage, *Bioscience*, 49, 29-37, 1999.
- 570 Berman-Frank, I., Rosenberg, G., Levitan, O., Haramaty, L., and Mari, X.: Coupling between
571 autocatalytic cell death and transparent exopolymeric particle production in the marine
572 cyanobacterium *Trichodesmium*, *Environmental microbiology*, 9, 1415-1422, 2007.
- 573 Berthelot, H., Moutin, T., L'Helguen, S., Leblanc, K., H  lias, S., Grosso, O., Leblond, N.,
574 Charri  re, B., and Bonnet, S.: Dinitrogen fixation and dissolved organic nitrogen fueled
575 primary production and particulate export during the VAHINE mesocosm experiment (New
576 Caledonia lagoon), *Biogeosciences*, 12, 4099-4112, 10.5194/bg-12-4099-2015, 2015.
- 577 Biegala, I. C., and Raimbault, P.: High abundance of diazotrophic picocyanobacteria (< 3   m)
578 in a Southwest Pacific coral lagoon, *Aquatic microbial ecology*, 51, 45-53, 2008.
- 579 Bonnet, S., Berthelot, H., Turk-Kubo, K., Fawcett, S., Rahav, E., l'Helguen, S., and Berman-
580 Frank, I.: Dynamics of N₂ fixation and fate of diazotroph-derived nitrogen in a low nutrient

low chlorophyll ecosystem: results from the VAHINE mesocosm experiment (New Caledonia), *Biogeosciences*, 12, 19579-19626, doi:10.5194/bg-12-19579-2015, 2015.

Bonnet, S., Moutin, T., Rodier, M., Grisoni, J. M., Louis, F., Folcher, E., Bourgeois, B., Boré, J. M., and Renaud, A.: Introduction to the project VAHINE: Variability of vertical and trophic transfer of diazotroph derived N in the South West Pacific, *Biogeosciences*, doi:10.5194/bg-2015-615, 2016.

Brussaard, C., Mari, X., Van Bleijswijk, J., and Veldhuis, M.: A mesocosm study of *Phaeocystis globosa* (Prymnesiophyceae) population dynamics: II. Significance for the microbial community, *Harmful algae*, 4, 875-893, 2005.

Capone, D. G.: Marine nitrogen fixation: what's the fuss?, *Curr. Opin. Microbiol.*, 4, 341-348, 2001.

Duhamel, S., Zeman, F., and Moutin, T.: A dual-labeling method for the simultaneous measurement of dissolved inorganic carbon and phosphate uptake by marine planktonic species, *Limnology and Oceanography-Methods*, 4, 416-425, 2006.

Dupouy, C., Neveux, J., Subramaniam, A., Mulholland, M. R., Montoya, J. P., Campbell, L., Capone, D. G., and Carpenter, E. J.: Satellite captures *Trichodesmium* blooms in the SouthWestern Tropical Pacific., *EOS, Trans American Geophysical Union.*, 81, 13-16, 2000.

Engel, A.: The role of transparent exopolymer particles (TEP) in the increase in apparent particle stickiness (α) during the decline of a diatom bloom, *Journal of Plankton Research*, 22, 485-497, 2000.

Engel, A., and Passow, U.: Carbon and nitrogen content of transparent exopolymer particles (TEP) in relation to their Alcian Blue adsorption, *Marine Ecology Progress Series*, 219, 1-10, 2001.

Engel, A., Goldthwait, S., Passow, U., and Alldredge, A.: Temporal decoupling of carbon and nitrogen dynamics in a mesocosm diatom bloom, *Limnology and Oceanography*, 47, 3, 753-761, 2002.

Engel, A.: Distribution of transparent exopolymer particles (TEP) in the northeast Atlantic Ocean and their potential significance for aggregation processes, *Deep-Sea Research Part I-Oceanographic Research Papers*, 51, 83-92, 2004.

Engel, A., Harlay, J., Piontek, J., and Chou, L.: Contribution of combined carbohydrates to dissolved and particulate organic carbon after the spring bloom in the northern Bay of Biscay (North-Eastern Atlantic Ocean), *Continental shelf research*, 45, 42-53, 2012.

Eppley, R. W., and Peterson, B. J.: Particulate organic-matter flux and planktonic new production in the deep ocean, *Nature*, 282, 677-680, 10.1038/282677a0, 1979.

Falkowski, P. G.: Evolution of the nitrogen cycle and its influence on the biological sequestration of CO₂ in the ocean, *Nature*, 387, 272-275, 1997.

Fukao, T., Kimoto, K., and Kotani, Y.: Production of transparent exopolymer particles by four diatom species, *Fisheries science*, 76, 755-760, 2010.

García, C., Prieto, L., Vargas, M., Echevarría, F., Garcia-Lafuente, J., Ruiz, J., and Rubin, J.: Hydrodynamics and the spatial distribution of plankton and TEP in the Gulf of Cadiz (SW Iberian Peninsula), *Journal of Plankton Research*, 24, 817-833, 2002.

Garcia, N., Raimbault, P., and Sandroni, V.: Seasonal nitrogen fixation and primary production in the Southwest Pacific: nanoplankton diazotrophy and transfer of nitrogen to

624 picoplankton organisms, Marine Ecology-Progress Series, 343, 25-33, 10.3354/meps06882,
625 2007.

626 Grossart, H. P., Simon, M., and Logan, B. E.: Formation of macroscopic organic aggregates
627 (lake snow) in a large lake: The significance of transparent exopolymer particles, plankton,
628 and zooplankton, Limnology and Oceanography, 42, 1651-1659, 1997.

629 Hong, Y., Smith, W. O., and White, A. M.: Studies on transparent exopolymer particles (TEP)
630 produced in the ross sea (antarctica) and by *Phaeocystis antarctica* (prymnesiophyceae),
631 Journal of Phycology, 33, 368-376, 1997.

632 Hoppe, H. G.: Significance of exoenzymatic activities in the ecology of brackish water:
633 measurements by means of methylumbelliferyl-substrates. , Marine Ecology Progress Series,
634 11, 299-308, 1983.

635 Kirchman, D.: Leucine incorporation as a measure of biomass production by heterotrophic
636 bacteria, Handbook of methods in aquatic microbial ecology. Lewis, 509-512, 1993.

637 Knapp, A. N., Fawcett, S. E., Martinez-Garcia, A., Leblond, N., Moutin, T., and Sophie., B.:
638 Nitrogen isotopic evidence for a shift from nitrate- to diazotroph-fueled export production in
639 VAHINE mesocosm experiments, Biogeosciences Discuss., 12, 19901-19939,
640 doi:10.5194/bg-12-19901-2015, 2015.

641 Leblanc, K., Cornet, V., Caffin, M., Rodier, M., Desnues, A., Berthelot, H., Turk-Kubo, K.,
642 and Heliou, J.: Phytoplankton community structure in the VAHINE mesocosm experiment,
643 Biogeosciences Discuss., doi:10.5194/bg-2015-605, 2016.

644 Logan, B. E., Passow, U., Alldredge, A. L., Grossartt, H.-P., and Simont, M.: Rapid formation
645 and sedimentation of large aggregates is predictable from coagulation rates (half-lives) of
646 transparent exopolymer particles (TEP), Deep Sea Research Part II: Topical Studies in
647 Oceanography, 42, 203-214, 1995.

648 Mari, X., and Burd, A.: Seasonal size spectra of transparent exopolymeric particles (TEP) in a
649 coastal sea and comparison with those predicted using coagulation theory, Marine Ecology-
650 Progress Series, 163, 63-76, 1998.

651 Mari, X., Beauvais, S., Lemée, R., and Pedrotti, M. L.: Non-Redfield C: N ratio of transparent
652 exopolymeric particles in the northwestern Mediterranean Sea, Limnology and
653 Oceanography, 46, 1831-1836, 2001.

654 Mari, X., Kerros, M. E., and Weinbauer, M. G.: Virus attachment to transparent exopolymeric
655 particles along trophic gradients in the southwestern lagoon of New Caledonia, Applied and
656 Environmental Microbiology, 73, 5245-5252, 10.1128/aem.00762-07, 2007.

657 Mohr, W., Grosskopf, T., Wallace, D. W., and LaRoche, J.: Methodological underestimation
658 of oceanic nitrogen fixation rates, PLOS one, 5, e12583, 2010.

659 Moisander, P. H., Serros, T., Paerl, R. W., Beinart, R. A., and Zehr, J. P.:
660 Gammaproteobacterial diazotrophs and nifH gene expression in surface waters of the South
661 Pacific Ocean, The ISME journal, 8, 1962-1973, 2014.

662 Moutin, T., Thingstad, T. F., Van Wambeke, F., Marie, D., Slawyk, G., Raimbault, P., and
663 Claustre, H.: Does competition for nanomolar phosphate supply explain the predominance of
664 the cyanobacterium *Synechococcus*?, Limnology and Oceanography, 47, 1562-1567, 2002.

665 Moutin, T., Van Den Broeck, N., Beker, B., Dupouy, C., Rimmelin, P., and Le Bouteiller, A.:
666 Phosphate availability controls *Trichodesmium* spp. biomass in the SW Pacific Ocean, Marine
667 Ecology-Progress Series, 297, 15-21, 2005.

668 Mulholland, M. R., and Capone, D. G.: The nitrogen physiology of the marine N₂-fixing
669 cyanobacteria *Trichodesmium* spp, Trends in plant science, 5, 148-153, 2000.

670 Ortega-Retuerta, E., Reche, I., Pulido-Villena, E., Agustí, S., and Duarte, C. M.: Uncoupled
671 distributions of transparent exopolymer particles (TEP) and dissolved carbohydrates in the
672 Southern Ocean, Marine chemistry, 115, 59-65, 2009.

673 Passow, U., and Alldredge, A. L.: A dye binding assay for the spectrophotometric
674 measurement of transparent exopolymer particles (TEP), Limnol. & Oceanogr, 40, 1326-
675 1335, 1995.

676 Passow, U.: Transparent exopolymer particles (TEP) in aquatic environments, Progress in
677 Oceanography, 55, 287-333, 2002.

678 Postgate, J. R., and Eady, R. R.: The evolution of biological nitrogen fixation, in: Nitrogen
679 Fixation: One Hundred Years After, edited by: Bothe, H., DeBruijn, F. J., Newton, W.E,
680 Gustav Fischer, Stuttgart, 31-40., 1988.

681 Prieto, L., Navarro, G., Cozar, A., Echevarria, F., and García, C. M.: Distribution of TEP in
682 the euphotic and upper mesopelagic zones of the southern Iberian coasts, Deep Sea Research
683 Part II: Topical Studies in Oceanography, 53, 1314-1328, 2006.

684 Radić, T., Degobbi, D., Fuks, D., Radić, J., and Đakovac, T.: Seasonal cycle of transparent
685 exopolymer particles' formation in the northern Adriatic during years with (2000) and without
686 mucilage events (1999), Fresenius environmental bulletin, 14, 224-230, 2005.

687 Rahav, E., Bar-Zeev, E., Ohayion, S., Elifantz, H., Belkin, N., Herut, B., Mulholland, M. R.,
688 and Berman-Frank, I. R.: Dinitrogen fixation in aphotic oxygenated marine environments,
689 Frontiers in Microbiology, 4, 10.3389/fmicb.2013.00227, 2013.

690 Rahav, E., Herut, B., Mulholland, M. R., Belkin, N., Elifantz, H., and Berman-Frank, I.:
691 Heterotrophic and autotrophic contribution to dinitrogen fixation in the Gulf of Aqaba,
692 Marine Ecology Progress Series, 522, 67-77, 2015.

693 Rochelle-Newall, E., Torretón, J.-P., Mari, X., and Pringault, O.: Phytoplankton-
694 bacterioplankton coupling in a subtropical South Pacific coral reef lagoon, Aquatic Microbial
695 Ecology, 50, 221, 2008.

696 Rodier, M., and Le Borgne, R.: Population dynamics and environmental conditions affecting
697 *Trichodesmium* spp. (filamentous cyanobacteria) blooms in the south-west lagoon of New
698 Caledonia, Journal of Experimental Marine Biology and Ecology, 358, 20-32,
699 10.1016/j.jembe.2008.01.016, 2008.

700 Rodier, M., and Le Borgne, R.: Population and trophic dynamics of *Trichodesmium thiebautii*
701 in the SE lagoon of New Caledonia. Comparison with *T. erythraeum* in the SW lagoon,
702 Marine Pollution Bulletin, 61(7-12), 349-359, 10.1016/j.marpolbul.2010.06.018, 2010.

703 Smith, D. C., and Azam, F.: A simple, economic method for measuring bacterial protein
704 synthesis rates in seawater using ³H-leucine Mar. Microb. Food Webs, 6, 107-114, 1992.

705 Spungin, D., Pfreundt, U., Berthelot, H., Bonnet, S., Al-Roumi, D., Natale, F., Hess, W. R.,
706 Bidle, K. D., and Berman-Frank, I.: Mechanisms of *Trichodesmium* bloom demise within the

707 New Caledonia Lagoon during the VAHINE mesocosm experiment, Biogeosciences Discuss.,
708 doi:10.5194/bg-2015-613, 2016.

709 Stam, H., Stouthamer, A. H., and van Verseveld, H. W.: Hydrogen metabolism and energy
710 costs of nitrogen fixation, FEMS Microbiology Reviews, 46, 73-92, 1987.

711 Stoderegger, K. E., and Herndl, G. J.: Production of exopolymer particles by marine
712 bacterioplankton under contrasting turbulence conditions, Marine Ecology Progress Series,
713 189, 9-16, 1999.

714 Tedetti, M., Marie, L., Röttgers, R., Rodier, M., Van Wambeke, F., Helias, S., Caffin, M.,
715 Cornet-Barthaux, V., and Dupouy, C.: Evolution of dissolved and particulate chromophoric
716 materials during the VAHINE mesocosm experiment in the New Caledonian coral lagoon
717 (South West Pacific), Biogeosciences Discuss., 12, 17453-17505, doi:10.5194/bgd-12-17453-
718 2015, 2015.

719 Thurman, E.: Organic Geochemistry of Natural Waters, Martinus Nijhoff/Dr W. Junk
720 Publishers, Dordrecht, 1985.

721 Turk-Kubo, K., Frank, I., Hogan, M., Desnues, A., Bonnet, S., and Zehr, J.: Diazotroph
722 community succession during the VAHINE mesocosm experiment (New Caledonia lagoon),
723 Biogeosciences, 12, 7435-7452, doi:10.5194/bg-12-7435-2015, 2015.

724 Urbani, R., Magaletti, E., Sist, P., and Cicero, A. M.: Extracellular carbohydrates released by
725 the marine diatoms *Cylindrotheca closterium*, *Thalassiosira pseudonana* and *Skeletonema*
726 *costatum*: Effect of P-depletion and growth status, Science of the Total Environment, 353,
727 300-306, 2005.

728 Van Wambeke, F., Pfreundt, U., Barani, A., Berthelot, H., Moutin, T., Rodier, M., Hess,
729 W.R., and S, B.: Heterotrophic bacterial production and metabolic balance during the
730 VAHINE mesocosm experiment in the New Caledonia lagoon, Biogeosciences, 12, 19861-
731 19900, doi:10.5194/bgd-12-19861-2015, 2015.

732 Verdugo, P., and Santschi, P. H.: Polymer dynamics of DOC networks and gel formation in
733 seawater, Deep Sea Research Part II: Topical Studies in Oceanography, 57, 1486-1493, 2010.

734 Verdugo, P.: Marine microgels, Annual review of marine science, 4, 375-400, 2012.

735 Villacorte, L. O., Ekowati, Y., Calix-Ponce, H. N., Schippers, J. C., Amy, G. L., and
736 Kennedy, M. D.: Improved method for measuring transparent exopolymer particles (TEP) and
737 their precursors in fresh and saline water, Water research, 70, 300-312, 2015.

738 Wood, A., and Van Valen, L.: Paradox lost? On the release of energy-rich compounds by
739 phytoplankton, Microbial Food Webs, 4, 103-116, 1990.

740 Wurl, O., Miller, L., and Vagle, S.: Production and fate of transparent exopolymer particles in
741 the ocean, Journal of Geophysical Research: Oceans (1978-2012), 116, 2011.

742 Zehr, J. P., and Kudela, R. M.: Nitrogen Cycle of the Open Ocean: From Genes to
743 Ecosystems, in: Annual Review of Marine Science, Vol 3, Annual Review of Marine Science,
744 197-225, 2011.

745 Zhou, J., Mopper, K., and Passow, U.: The role of surface-active carbohydrates in the
746 formation of transparent exopolymer particles by bubble adsorption of seawater, Limnology
747 and Oceanography, 43, 1860-1871, 1998.

748 Ziervogel, K., D'souza, N., Sweet, J., Yan, B., and Passow, U.: Natural oil slicks fuel surface
749 water microbial activities in the northern Gulf of Mexico, Frontiers in microbiology, 5, 2014.

750

751

Figure legends

Figure 1. Temporal changes in transparent exopolymeric particle (TEP) concentrations ($\mu\text{g GX L}^{-1}$) during the VAHINE mesocosm experiment. Data shown are from daily sampling of three depths (1, 6, 12 m) in each mesocosm. Data was analyzed according to the characterized phases of the experiment based on the diazotrophic communities that developed in the mesocosms (Turk-Kubo et al., 2015) and biogeochemical characteristics (Bonnet et al., 2015). **a.** Mesocosm 1 (M1) **b.** Mesocosm 2 (M2), **c.** Mesocosm 3 (M3), **d.** samples from the lagoon waters outside of the mesocosms (O). Phases: P0= days 2-4, P1= days 5-14, P2= days 15-23. Linear regressions (Pearson) of TEP for each of the phases are designated by a solid line, only when significant. Pearson correlations coefficients and significant values ($p < 0.05$) are represented in bold in Table S1.

Figure 2. Total content of transparent exopolymeric particles (TEP) per mesocosm and in the lagoon waters surrounding the mesocosms. The average amount in $\text{g GX mesocosm}^{-1}$ for the two periods of the experiment after DIP fertilization was calculated from the total daily amount based on concentrations measured at three depths and integrated for the specific volume per mesocosm or for an equivalent volume of lagoon water. Averages are represented in boxplots as a function of two different phases: P1 = days 5-14 and P2 = days 15-23. Red (mesocosm 1 - M1), blue (mesocosm 2- M2), green (mesocosm - M3) and black (Outside lagoon O). Straight lines within the boxes mark the median. No significant differences were observed between the phases or between the three mesocosms and the outside lagoon (Kruskal-Wallis non-parametric analysis of variance; $p > 0.05$).

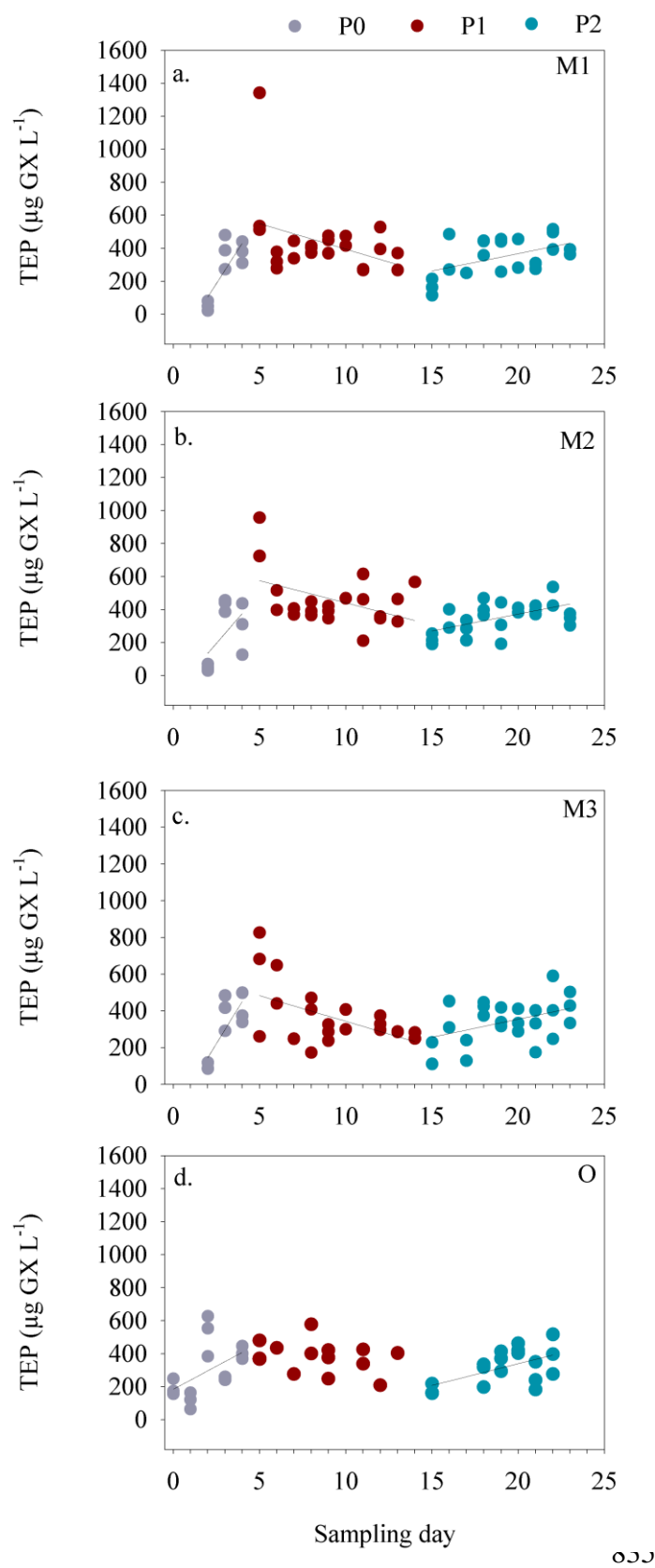
Figure 3. Relationships between the concentration of transparent exopolymeric particles (TEP), ($\mu\text{g GX L}^{-1}$) and **a.** dissolved inorganic phosphorus DIP ($\mu\text{mol L}^{-1}$), **b.** turnover time of DIP - T_{DIP} (d) and **c.** alkaline phosphatase activity (APA), ($\text{nmol L}^{-1} \text{ h}^{-1}$) in the three mesocosms (M1-red; M2-blue; M3-green) during phase 2 (days 15-23). For a and b Pearson linear regressions yielded an $R^2 = 0.54$, $n = 23$ (TEP/DIP) and an $R^2 = 0.52$, $n = 26$ (TEP/ T_{DIP}), and for c. Log-transformed ($\log(\text{TEP}) / \log(\text{APA})$) with $R^2 = 0.68$, $n = 25$. All correlations were significant ($p < 0.05$). Error bars represent ± 1 standard deviation.

Figure 4. a. Temporal dynamics of TEP carbon concentrations (TEP-C, μM) in relationship to the average total organic carbon (TOC), ($\mu\text{g L}^{-1}$), (thin black line) in the mesocosms (M1-red dots, M2-blue dots, M3-green dots, and black dots- Outside waters (O). Black solid line designates TEP-C averaged for the three mesocosms (thick black line). TEP-C was measured

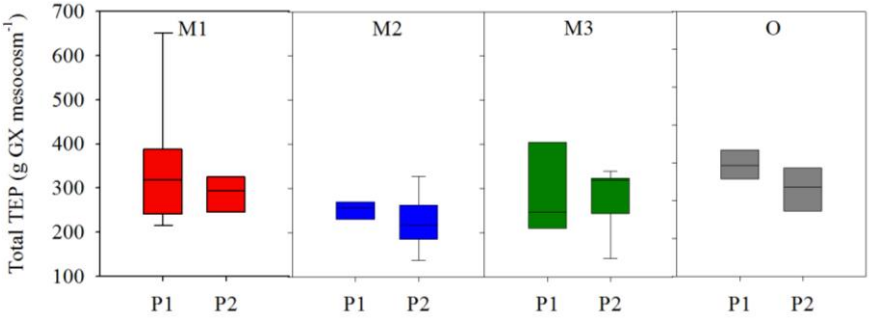
from 6 m depths and calculated according to Engel (2000). **b.** Temporal changes in the percent of TEP-C from TOC (%) in mesocosms (green dots), and %TEP-C in the lagoon waters (Out), (black dots). **c.** Relationship between TEP concentrations ($\mu\text{g GX L}^{-1}$) and TOC ($\mu\text{mole L}^{-1}$), during phase 2 (days 15-23) for Mesocosm 1 (M1, red dots), Mesocosm 2 (M2, blue dots), Mesocosm 3 (M3, green dots). Significant correlations were observed (Pearson) for all mesocosms. $R^2 = 0.75\text{-M1}$, 0.73-M2 , and 0.58-M3 respectively, $n=7\text{-}8$, $p < 0.05$. All statistics are detailed in Table S2, ($p=0.05$, $n= 7\text{-}8$). Error bars represent ± 1 standard deviation.

Figure 5. Relationship between heterotrophic bacterial production (BP), ($\text{ng C L}^{-1} \text{ h}^{-1}$) and TEP concentrations ($\mu\text{g GX L}^{-1}$) during phase 2 (days 15-23) when BP increased following the enhanced PP (Van Wambeke et al., 2015), for Mesocosm 1 (M1, red dots), Mesocosm 2 (M2, blue dots), Mesocosm 3 (M3, green dots). Pearson's linear regressions yielded $R^2 = 0.57$ for M1, 0.42 for M2, and 0.56 for M3 respectively. Significant correlations were observed for all mesocosms and are detailed in Table S2. Error bars represent ± 1 standard deviation.

Figure 6. Temporal changes in TEP concentrations and Het-1 net growth rates (d^{-1}), (gray triangles) for **a.** Mesocosm 1 (M1) **b.** Mesocosm 2 (M2), **c.** Mesocosm 3 (M3). TEP concentrations were averaged from the three depths sampled per mesocosm (green circles). Het-1 net growth rates were calculated based on changes of *nifH* copies L^{-1} (Turk-Kubo et al., 2015) measured every other day. **d.** Relationship between TEP concentrations ($\mu\text{g GX L}^{-1}$) and Het-1 growth rate (d^{-1}) for all three mesocosms. Significant correlations were observed (Pearson) from all mesocosms together. $R^2 = 0.60$, $p = 0.0001$, $n = 19$. Error bars represent ± 1 standard deviation. **e-f.** Epifluorescent microscopical images of the diatom-diazotroph association *Richelia-Rhizosolenia* identified by Het-1 abundance. Images by V. Cornet-Barthaux. **g-h.** the diazotroph UCYN-C which bloomed and formed large aggregates (comprised also of TEP) that enhanced vertical flux and export production during P2. Images by S. Bonnet.



837 **Figure 2**



844

845

846

847

848

849

850

851

852

853

Figure 3

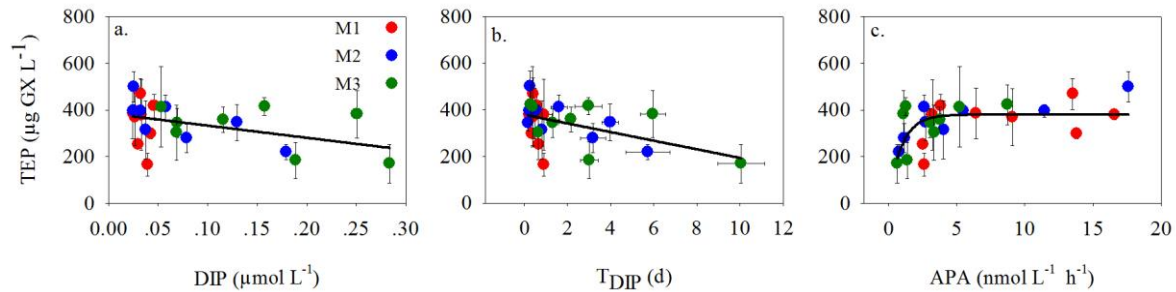


Figure 4

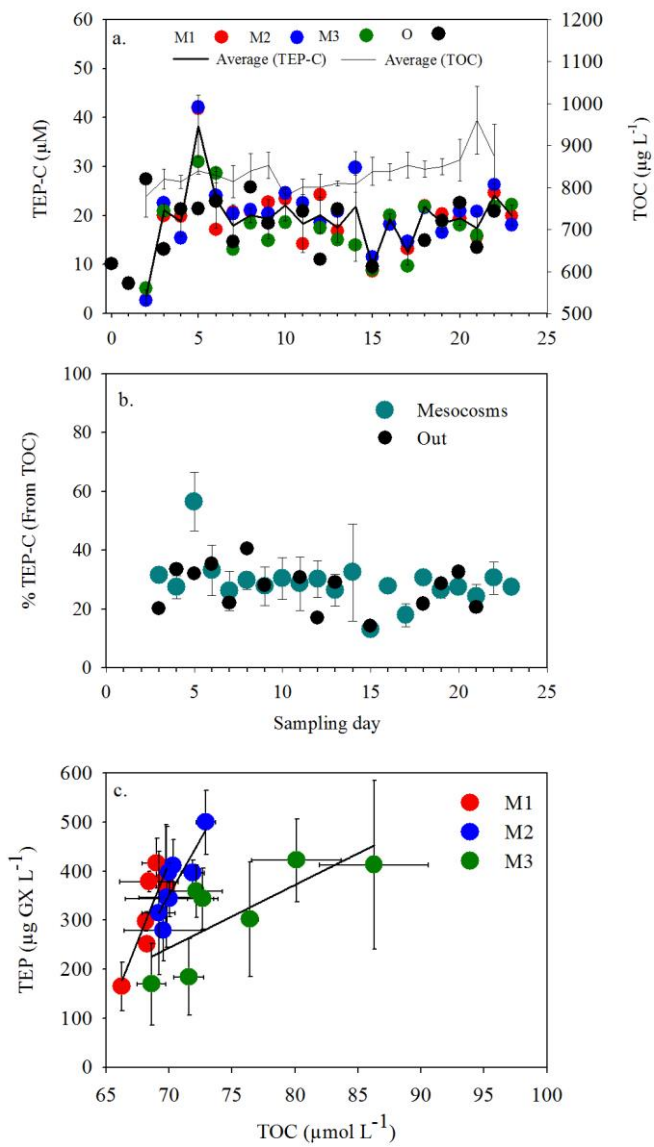


Figure 5

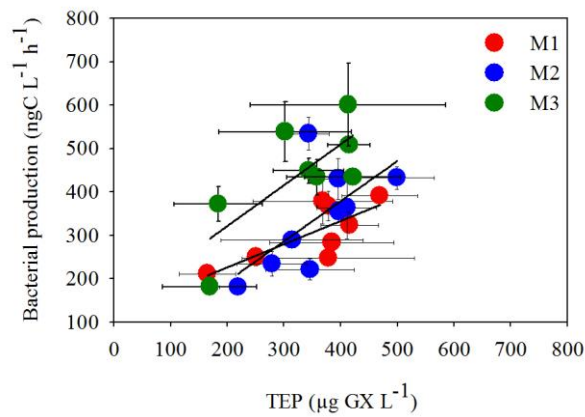


Figure 6

